Supplementary material

A novel method for measuring tension generated in stress fibers by applying external forces

Shukei Sugita, Taiji Adachi, Yosuke Ueki, and Masaaki Sato

Effect of stretching and bending on the measured tension

The method proposed in this study measures the displacement of individual SFs by applying an external force perpendicular to the fiber axis. Although the method enables us to measure tensions, it also generates other undesired forces in the SFs due to phenomena such as stretching and bending. Here, we estimate the stretching and bending forces and analyze the effects of these undesired forces on the measured tensions in SFs.

The SFs are assumed to have a cylindrical shape and elastic mechanical properties. The geometrical parameters associated with the tension measurements are shown in Fig. S1. When an external force F is applied perpendicular to the SF axis, the SF becomes stretched as shown in Fig. S2 *A*, where F_S represents the stretching force. Considering the left part of the SF, the strain, ε_L, due to the stretching is expressed as

$$\varepsilon_L = \frac{1-\cos\theta_L}{\cos\theta_L} . \tag{S1}$$

The force F_S can then be written as

$$F_S = A_L \varepsilon_L E = \pi r_{SF}{}^2 E \frac{1-\cos\theta_L}{\cos\theta_L} , \tag{S2}$$

where A_L is the cross-sectional area, r_{SF} the cross-sectional radius, and E is the elastic modulus of the SF. Substituting θ_L = 5°, which is typical of the values measured in this study, and r_{SF} = 100 nm and E = 0.5 MPa from the literature (1) gives an estimated force due to stretching of F_S = 60 pN. This is about 4% of the measured tension of 1.6 nN; therefore, the effect of stretching on the tension measurements is considered negligible.

When an SF is bent by an external force F, it is opposed by a repulsive force F_R due to the bending rigidity of the SF (Fig. S2 *B*). The displacement, y, at the point of application of the external force is given by

$$y = \frac{F_R a^2 b^2}{3EI(a+b)} = a \cdot \tan\theta_L, \tag{S3}$$

where a and b are the lengths of the left and right sections of the SF, respectively, and I is moment of inertia, which can be written as

$$I = \frac{\pi r^2}{4}. \tag{S4}$$

Substituting typical measured values of a = b = 2.5 μm and θ_L = 5°, and values of r_{SF} and E from the literature, Eq. S3 gives an estimated repulsive force of F_R = 3.3 pN. Because the repulsive force due to bending is just a few percent of the applied external force of several hundred piconewtons, the effect of the bending on the tension measurements is also considered to be negligible.

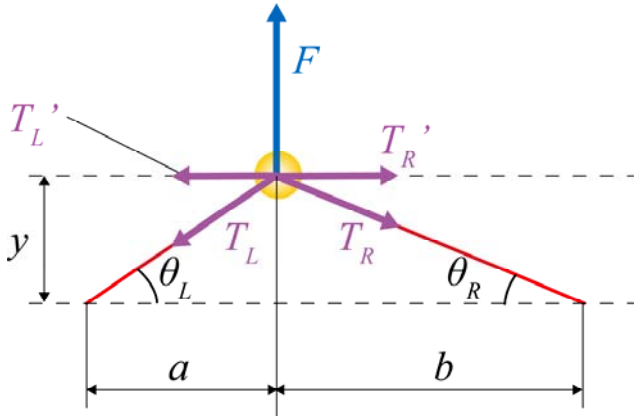

Fig. S1 Geometrical parameters when an external force, F, is applied perpendicular to the fiber (*red*). The ball (*yellow*) represents a magnetic particle bound to the fiber.

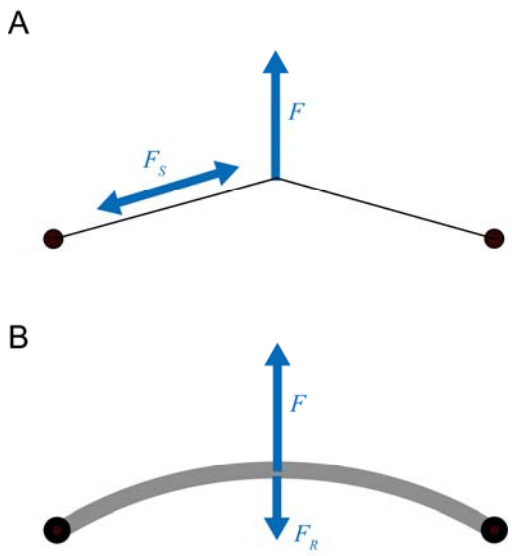

Fig. S2 Schematic illustration of extra, undesired forces (F_S, F_R) generated in a fiber due to (*A*) stretching and (*B*) bending, both of which are caused by the external force, *F*.

Effect of rotation of magnetic bead

The bead shown in Fig. 5 may have rotated when the magnetic force was applied. Here, we will show that rotation of the beads would have no significant effect on the tension measurements.

Fig. S3 shows a schematic diagram of a filament and bead before and after the application of a magnetic force *F*. Fig. S3, *A* and *B* show top views and Fig. S3, *C*–*E* show axial views. We now consider the balance of forces and moments in 3-dimensional space. Since the magnetic force acting on the bead is a body force, it acts on the center of the bead. When a magnetic force *F* is applied to the bead (Fig. S3, *A* and *C*), the bead moves toward the tip of the magnetic needle until the magnetic force balances the tension T_L and T_R (Fig. S3 *B*). The method proposed for measuring tension in SFs in this study utilizes this static force balance. When the applied force *F* and tensions T_L and T_R are considered from the axial view, angular momentum is generated because *F* is acting along a different axis to T_L and T_R, as shown in Fig. S3 *D*. Thus, the bead undergoes rotation (thick black arrow in Fig. S3 *D*). Since the bead is bound to the SF, this rotation twists the SF, resulting in the application of a reactive moment ($-M_t$) to the bead by the SF in order to try to recover the untwisted state. Therefore, the bead rotates through an angle φ until this reactive moment

balances the moment produced by F, T_L, and T_R. Here, it should be emphasized that although the angular momentum is generated because F, T_R, and T_L are not acting along the same axis, no change occurs in the force balance. That is, no additional forces are generated. During rotation, the forces do not change their magnitude or direction but only their relative position. It should be also noted that the deformation of the filament was measured not from the bead displacement but from the orientations of both ends of the SF. Therefore, the tension measurements carried out in this study, using only the force balance, are not affected by rotation of the bead.

Furthermore, the force component causing rotation of the bead was found to be small. When both forces and moments are balanced by bead rotation through an angle φ, the force F_t, which is the component of F that contributes to the moment about the center of the SF (point O in Fig. S3 *E*), can be estimated. The tension T_L, and T_R does not generate the moment, and only F_t contribute to the moment (Fig. S3 *E*). The magnitude of the F_t was estimated as follows.

Under assumption that SFs are isotropic, linear, elastic cylindrical rod and incompressible, we firstly estimated the shear modulus G of the SFs from their elastic modulus E as

$$G = \frac{E}{2(1+\nu)}, \tag{S5}$$

where the ν is the Poisson's ratio and $\nu = 0.5$ under the incompressibility.

The polar moment of inertia I_P of area of SFs is

$$I_P = \frac{\pi r_{SF}^{\ 4}}{2}, \tag{S6}$$

where r_{SF} is cross-sectional radius of SFs. When the magnetic force was applied to the SF, the SFs should be twisted up to $\varphi = 90°$ at the maximum. The moment required to twist the SFs M_t is written as

$$M_t = \frac{GI_P\varphi}{L}, \tag{S7}$$

where, L is the length of the SF. Substituting L = 2.5 μm as representative value of this

study and r_{SF} = 100 nm and E = 0.5 MPa from the literature (1), M_t is estimated as

$$M_t = 1.6 \times 10^{-17} \text{ (Nm)}.$$

Since the radius of the magnetic beads r_{mb} is 1.4μm, the force F_t is calculated as

$$F_t = 1.2 \times 10^{-11} \text{ (N)}.$$

The force to rotate the beads F_t is only ~1% of the magnitude of the applied force F. Therefore, even though the bead rotates, the rotation has no significant effect on the force measurement since the contribution of the force is small.

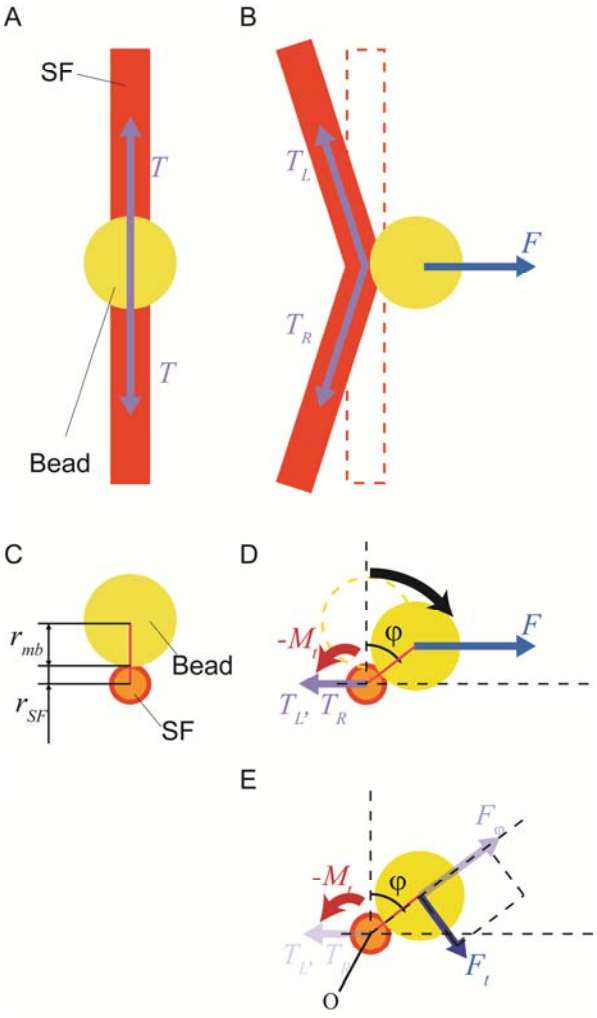

Fig. S3 Schematic illustration of balance of forces and moments for an SF bound to a magnetic bead (*A*,*B*: top view; *C*–*E*: axial view). Figures (*A*) and (*C*) represent the situation before force application and (*B, D,* and *E*) following force application. In (*E*), only the force element contributing to the moment around point O is thickly drawn. The force F_t and F_φ

are components of the applied force F.

Effect of existence of more anchor or bifurcation points among the observed single SF.

Typical length of SFs measured in this study was ~10 μm. However, there might be thin and invisible between clearly visible SFs. We estimated the effects of such an existence of thin and invisible SFs on the tension measurement.

Fig. S4 shows a schematic illustration of a thin invisible SF (SF_{2R}) between visible SFs (SF_{1L} and SF_{2L}). If a thin SF SF_{2R} exists, the equations of force balance among T_{1L}, T_{2L}, and T_{2R} (* in Fig. S4) are written as

$$T_{1L}\sin\theta_{1L} = T_{2L}\sin\theta_{2L} + T_{2R}\sin\theta_{2R} \quad \text{(S8)}$$

$$T_{1L}\cos\theta_{1L} + T_{2R}\cos\theta_{2R} = T_{2L}\cos\theta_{2L}. \quad \text{(S9)}$$

From Eq. S9,

$$T_{2L} = \frac{1}{\cos\theta_{2L}}\left(T_{1L}\cos\theta_{1L} + T_{2R}\cos\theta_{2R}\right). \quad \text{(S10)}$$

By substituting Eq. S10 into Eq. S8, we obtain

$$T_{2R} = \frac{\sin\left(\theta_{1L} - \theta_{2L}\right)}{\sin\left(\theta_{2L} + \theta_{2R}\right)}T_{1L}. \quad \text{(S11)}$$

By substituting Eq. S11 into Eq. S9, we obtain

$$T_{2L} = \frac{\sin\left(\theta_{1L} + \theta_{2R}\right)}{\sin\left(\theta_{2L} + \theta_{2R}\right)}T_{1L}. \quad \text{(S12)}$$

If SF_{1L} and SF_{2L} appear as a single SF, i.e., the SF_{1L} and SF_{2L} appear straight, then

$$\theta_{1L} \approx \theta_{2L}. \quad \text{(S13)}$$

Therefore, we obtain the following equation by substituting Eq. S13 into Eqs. S11 and S12.

$$T_{2R} \approx 0$$

$$T_{2L} \approx T_{1L}.$$

This result shows that even if there are thin invisible SFs connecting the visible SFs, this would have no significant effect on the measured tension if the visible SF appeared straight.

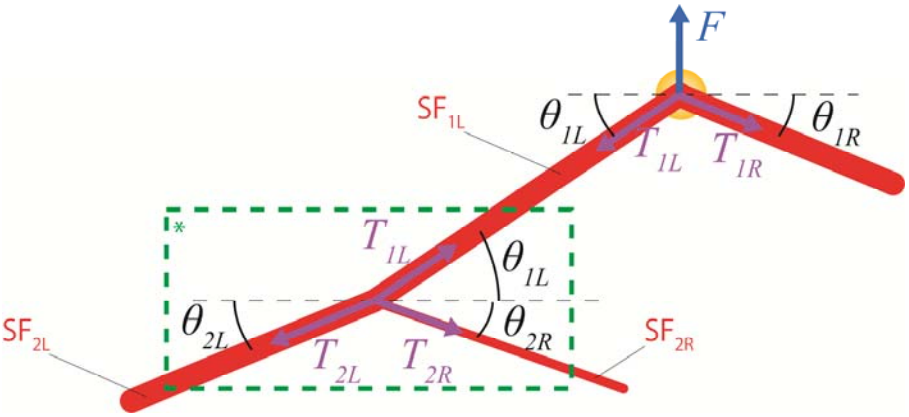

Fig. S4 Schematic illustration of SFs (SF_{1L}, SF_{2L}, and SF_{2R}) during application of a force *F*. At area *, a balance should exist among the tensions within SFs.

The linearity of the SF was then investigated by reducing the number of myosin points that were used for linear regression to determine the SF angle. Fig. S5 shows a tension analysis when the number of myosin points were reduced from the side furthest from the magnetic bead. The results show that the measured tension did not exhibit any unidirectional variation. If there were thin SFs between the clearly visible SFs, and the visible SFs were not straight (for example, if they had the typical quadratic shape of a bent beam), the measured tension shown in Fig. S5 should decrease with the number of points used because $\sin\theta_L$ and $\sin\theta_R$ in Eq. 3 increase. Therefore, we concluded that the SFs which we analyzed in this study were almost straight.

In conclusion, although the presence of thin SFs between the visible SFs is a possibility, they should have no significant effect on the tension if the visible SFs are almost straight, as we have shown to be the case. Therefore, the existence of additional anchor points should not seriously affect the measured tension.

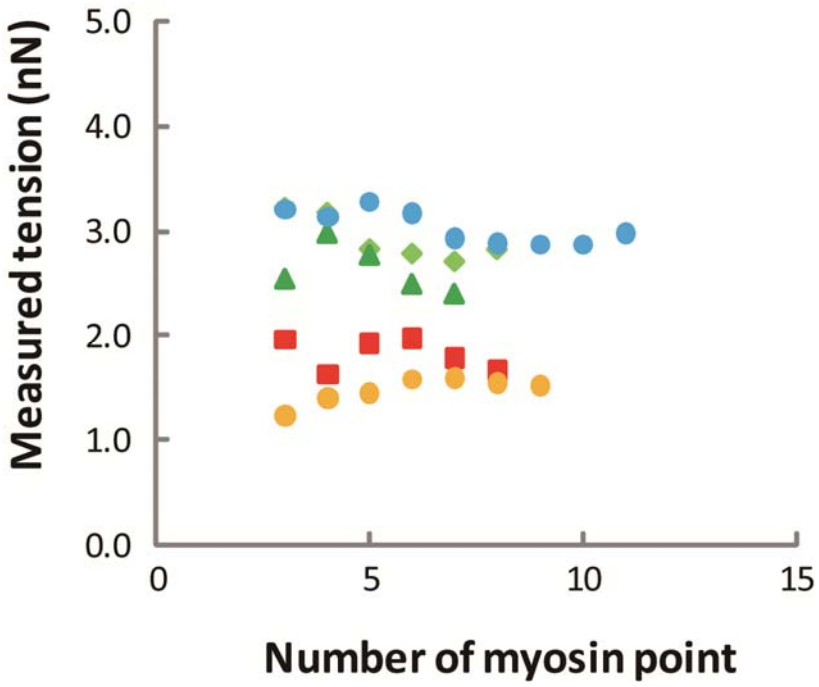

Fig. S5 Dependence of the measured tension on the number of myosin points used for linear regression to determine the SF bending angle.

Estimation of errors in measurement from the determination of myosin position

To investigate the error in Fig. 5 *K*, we measured the distance from the actual data points to the fitting line, and then obtained the error by dividing this by the fitting line value. This analysis was performed to show that it is reasonable to assume that errors in the myosin position are the source of the errors in the tension measurements. Fig. S6 shows the error distribution obtained using all 19 measured tension data. This is a normal distribution with a standard deviation (SD) of about 11%.

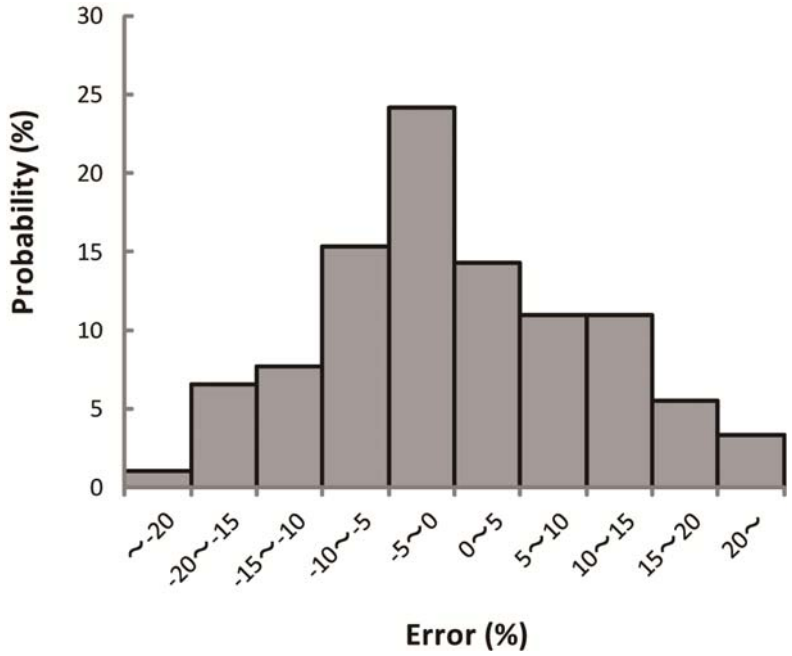

Fig. S6 Percentage error distribution of T' (tensions in the original filament direction during force application) in Fig. 5 *K*. Bars represent the probability of each error occurring.

In this study, the SF angles were determined from the positions of the fluorescent myosin labels. The error in the myosin positions is determined using a method that assumes a Poisson pixel noise distribution, as reported by Sbalzarini *et al* (2). Based on 19 measurements of myosin positions, the SD of the positional error was found to be ~0.1 pixel. Since the bending angle of the SF is determined from the positions of multiple myosins, it is difficult to directly determine the angular error from the myosin positional error. Therefore, we carried out a simulation to estimate the angular error. First, the center points of the myosin images obtained in this study were assumed to be the correct positions (*green points* in Fig. S7) and the resulting orientation of the SF (*green line* in Fig. S7) was determined as described in the Method section in this paper. The myosin positions were then statistically varied using a normal probability distribution with a SD of 0.1 pixel (*red points* in Fig. S7). The SF orientation was again evaluated (*red line* in Fig. S7) and the angular difference from the correct orientation (γ in Fig. S7) was measured. This process was repeated 1000 times for each SF. For the 19 tension measurements, the angle γ was found to be 0.0 ± 0.57° (mean ± SD), which is the error in the SF bending angle due to myosin positional errors.

Since, in this study, the SFs bent by 4.1° as average under the applied magnetic force, the error in the measured tension is 13%, which is comparable to the error in Fig. 5 *K* (SD = 11%). Therefore, the error in Fig. 5 *K* is thought to be mainly due to myosin positional errors.

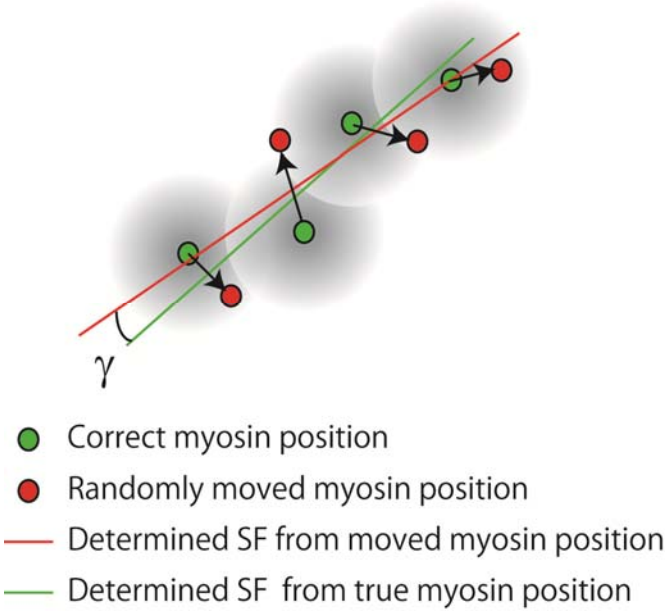

Fig. S7 Schematic illustration of a simulation for obtaining the angular error in the SF orientation due to myosin positional errors. The correct myosin positions were assumed to be those measured in this study. The new positions were assigned based on a normal probability distribution with a SD of 0.1 pixel.

References

1. Deguchi, S., T. Ohashi, and M. Sato. 2005. Evaluation of tension in actin bundle of endothelial cells based on preexisting strain and tensile properties measurements. Mol Cell Biomech 2:125-133.

2. Sbalzarini, I. F., and P. Koumoutsakos. 2005. Feature point tracking and trajectory analysis for video imaging in cell biology. Journal of Structural Biology 151:182-195.